Sindh Univ. Res. Jour. (Sci. Ser.) Vol.49 (004) 785-792 (2017)

http://doi.org/10.26692/sujo/2017.12.0058

SINDH UNIVERSITY RESEARCH JOURNAL (SCIENCE SERIES)

A Finite Element Analysis of Pore Throat Ratio on the Characteristics of Flow Structure through Low Permeability Reservoir

Z. A. BALOCH*, S. B. SHAH, H.SHAIKH** M. E. BALOCH***

Department of Petroleum Engineering, University of Stavanger, Norway.

Received 23rd January 2016 and Revised 17th November 2017

Abstract: Present research work focus on the two–dimensional axisymmetric incompressible flow of a Newtonian fluid through Pore–Throat tube. Different model parameters are employed to investigate the influence of inertia and impact of various pore throat ratios on flow structure, pressure differential, stress distribution and friction factor. A time–marching finite element method is used to analyse the numerical solutions through flow structure via streamline distribution, pressure distribution, speed and stress. A time–marching Taylor–Galerkin/Pressure–Correction procedure in semi–implicit form is employed to achieve the steady–state solutions. Predicted numerical results demonstrate Pore–Throat ratio have vital impact on the flow field distribution.

Keywords: Pore–Throat Tube, Finite Element Method, Newtonian Fluids, Flow in Porous Media, Low Permeability, Pore Structure.

1. INTRODUCTION

The flow of fluid in a low permeability porous media has great importance in the process of micro–scale (pore–scale). The numerical analysis of these flows has fascinated by the number of researchers. Since both fluid and porous media are continuous mediums and can be divided in to four different scales such as pore–scale, core–scale, mega–scale and giga–scale (Bear, 1972, Al–Raoush and Alshibli, 2006). As the problem of micro–scale issue is not fully understood, so far micro–scale is not clearly be defined and is comparatively scale model. Time–space of micro–scale varies in different areas of study. Space micro-scale is generally referred to huge scales (Harley, *et al*. 1995 and Fu–Quan, 2004). Usually it has ranges from micron to atomic, i.e. micron, submicron, Nano–metre, cluster and atom, and the maximum limit of micron range are below hundred µm. In devices, the application of micro–scale values may lead to order of scale increase in the region to volume ratios and in the cells of fuel, where in heat and mass transfer and electrochemical reactions, micro–scale principles can lead to major breakthrough in density of power, cost effectiveness (Mala, 1999 and Kandlikar, 2002). The submicron can be defined as the size in between 0.1µm and 1nm and the scale which haslarge size about 1mm is referred as macroscopic scale, while has ranges from 1µm up to 1 mm is defined as micro–scale.

Recently, number of researchers studied on the fluid flow in the area of low permeability of porous matrix (Gravesen, *et al*. 1993, Fu–Quan, 2004, Jicheng, (2010), Shaikh, (2012 and 2013). The flow through low permeability porous material of fluid is purely referred as micro–scale flow phenomena, such as Jicheng, *et al*. (2010) investigated the appearances of fluid flow through Expansion–contraction Channel of Low Permeability Reservoir. The two–dimensional Newtonian model presented to express the flows of velocity, speed and stream functions and various computations of the models such as effects of same pore radius, various throat radius and change in pore radius were analysed. Jicheng, *et al*. (2010) concluded that effects of throat radius and various ratios of pore throat were highly showed the effects on the fluid flow distributions but small variations are examined with the influences of pore length.

2. Problem Specification

An incompressible flow of Newtonian fluid within Pore–Throat tube is analysed as a region of the interest. Whilst, flow is assumed to be axisymmetric inside circular tube, consequently, the upper–half of the geometry is considered. The domain of the flow is presented in **(Fig. 1)**. While the radius of the Pore–Throat circular geometry is calculated laterally in the axial flow direction via 'r_w' as:

$$r_w = R_s\left[1+\lambda\, Cos\left(\frac{2\pi z}{L_a}\right)\right] \quad (1)$$

Where, λ and L_a are respectively non–dimensional amplitude of Pore–Throat wave and wave length. While R_s is an average radius of plane circular domain

++Corresponding Author: Email: asadullah.khoso@gmail.com
** Department of Mathematics Shah Abdul Latif University, Khairpur
*** Department of Computer System Engineering Technical University Duisburg, Germany

(straight tube with unit radius). The coordinate system considered in this investigation is cylindrical polar coordinates (r, z), where r is a radial direction and $\boldsymbol{z}$-axis is an axial direction, along the axis of flow direction.

To state the well–posed problem, it is vital to describe both initial and as well as boundary conditions. Here mixed Dirichlet and Neumann boundary conditions considered as given in following **(Table–1)**:

Table–1: Initial and Boundary conditions for Momentum Transport Equation

Initial Conditions	**Quiescent flow condition $v_r(z,0) = v_z(r, 0) = 0$**
Boundary Conditions	1. $v_z = v_{\max}\left\{1-\left(\frac{r}{R_s}\right)^2\right\}$ and $v_r = 0$ condition is considered at inlet. 2. No-slip condition at solid wall: $v_r = v_z = 0$. 3. $v_r = p = 0$, and v_z is unknown at outlet. 4. $v_r = 0$ and $\frac{\partial v_z}{\partial r} = 0$ a traction free condition at axis of symmetry.

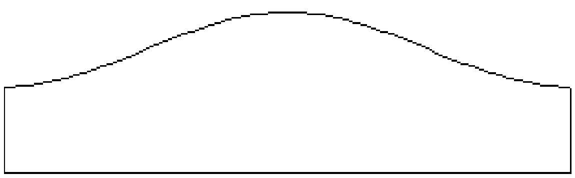

Figure–01: Computational domain for flow interest through Pore–Throat Tube.

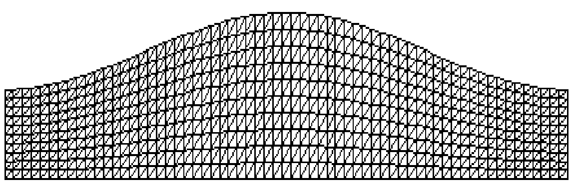

Coars Mesh

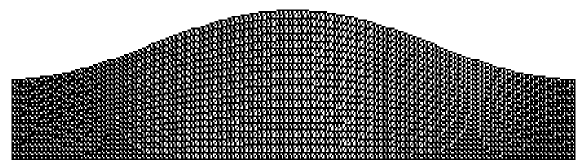

Refined Mesh

Fig. 2: Finite Element Meshes of Pore–Throat Tube.

3. System of governing equations

This investigation considers an incompressible flow of Newtonian fluid under isothermal condition within Pore–Throat tube. The flow is governed via continuity and momentum transport equations. The dimensionless system of equations in the polar coordinate system without considering body forces can be presented as:

Continuity equation:

$$\frac{1}{r}\frac{\partial}{\partial r}(r v_r) + \frac{\partial}{\partial z}(v_z) = 0 \tag{2}$$

Momentum Transport Equation:

$$\rho\left(\frac{\partial v_r}{\partial t} + v_r\frac{\partial v_r}{\partial r} + v_z\frac{\partial v_r}{\partial z} - \frac{v^2{}_\theta}{r}\right) = \left[\frac{1}{r}\frac{\partial}{\partial r}(r\tau_{rr}) + \frac{\partial}{\partial z}\tau_{zr} - \frac{\tau_{\theta\theta}}{r}\right] - \frac{\partial p}{\partial r} \tag{3}$$

$$\rho\left(\frac{\partial v_z}{\partial t} + v_r\frac{\partial v_z}{\partial r} + v_z\frac{\partial v_z}{\partial z}\right) = \left[\frac{1}{r}\frac{\partial}{\partial r}(r\tau_{rz}) + \frac{\partial}{\partial z}\tau_{zz}\right] - \frac{\partial p}{\partial z} \tag{4}$$

Where v_r and v_z are the non-dimensional velocity components of fluid material point in the radial and axial direction respectively, m/s; while, r and z are respectively radial and axial direction. Whilst ρ is the density of fluid material point, kg/m^3 and t is time (s).

As per actual range of low permeability wires, three different set of parameters for Pore–Throat tube flow models are analysed here. It has been observed that, Pore–Throat ratio and pore length of Pore–Throat tube flow exert on the flow line and shear stress distribution (Makihara, *et al*. 1993). In this particular investigation feature of fluid distribution in Pore–Throat tube flow is investigated at the conditions of different pore parameters.

3.2 Constitutional equation

The constitutional equation of Newtonian fluid in tensor form can be expressed as:

$$\boldsymbol{\tau}_{ij} = 2\mu_1\varepsilon_{ij} + \left(-p + \mu_2\nabla.\boldsymbol{v}\right)\delta_{ij} = \mu_1\left(\frac{\partial v_z}{\partial r} + \frac{\partial v_r}{\partial z}\right) + \left(-p + \mu_2\left(\frac{1}{r}\frac{\partial}{\partial r}(r v_r) + \frac{\partial v_z}{\partial z}\right)\right)\delta_{ij} \tag{5}$$

Here τ_{ij} be the stress tensor, ε_{ij} is the rate of strain tensor, m/t, μ_1 and μ_2 are the first and second viscosities of fluid, pa.s. ,*p* the pressure of fluid suffers, while δ_{ij} is the Kronekar delta and can be represented as:

$$\delta_{ij} = \begin{cases} 1 & i = j \\ 0 & i \neq j \end{cases} \qquad (6)$$

4. NUMERICAL ALGORITHM

For low permeability flows, a time–marching finite element method is employed to predict steady–state numerical solutions. In this regard a semi–implicit based Taylor–Galerkin/Pressure–Correction algorithm (Baloch, 1994, Baloch, *et al*. 1995 and Baloch and Memon, 2007) is employed**.** Originally, the scheme was built for complex flows of constant viscosity fluids in the time stepping framework (Qureshi and Baloch, 2013, Solangi, *et al*. 2013 and Shah, *et al*. 2013 and 2014). For completeness, the summary of the algorithm is described here. This scheme comprises temporal discretisation through Taylor series expansion combined with predicator–corrector scheme. Two steps Lax–Wendroff approach is adopted to achieve second order time derivatives (Baloch, *et al*. 2013, 2014). Pressure–correction technique ensures the second order accuracy and stability, when it is integrated with two–steps ,i.e., predicator and corrector steps, scheme in Taylor–Galerkin algorithm (Shaikh, *et al*. 2013 and 2014, Shah, 2013 and Solangi, 2013).For present numerical algorithm employed in this study, this approach also provides the bases to acquire the steady–state results.

To obtain the numerical solutions, a multi–step approach is adopted. Primarily, at first–step the solution is attained at half time step, whilst, as a second part of first–step, a transitional non–divergence–free velocity field is computed. While, at step–two pressure differential is evaluated by resolving the Poisson equation. To get the second order accuracy, Crank–Nicolson as a semi–implicit scheme is used (Baloch, *et al*. 2013, 2014 and Memon, *et al*. 2015). While, non–divergence–free velocity field is achieved at third step. First– and third–steps are structured by the augmented mass matrices, therefore both steps are computed iteratively, with a handful number of iteration, very efficiently, using modified Jacobi's iterative method. This technique circumvents the assembly of system matrix, which is helpful component to accelerate the solution process.

At step–two, direct Choleski's method is adopted to seek solution for pressure–differential, since the pressure difference stiffness matrix is symmetric, positive–definite and with banded structure. A Galerkin weighted residual technique is adopted. An integrated velocity and pressure formulation is employed, spatially, domain is distributed in triangular tessellation. For finite element approximation, over each element, equations are discretised using piecewise quadratic shape function for velocity and linear shape functions for pressure (Townsend, and Webster, 1987 and Baloch, 1994).

Stage–1(a): Compute velocity field at half time–step $v^{n+\frac{1}{2}}$ for given $\left(v^n, p^n\right)$, such that

$$\left\{\left(\frac{2}{\Delta t}\left(v^{n+\frac{1}{2}} - v^n\right), v\right) + \frac{1}{2\mathrm{Re}}\left(\nabla\left(\left(v^{n+\frac{1}{2}} - v^n\right), \nabla v\right)\right)\right\} \qquad (7)$$
$$= \left(-p^n - \frac{1}{\mathrm{Re}}\nabla v^n, \nabla v\right) - \left(\left((v.\nabla)v\right)^n, v\right)$$

Stage–1(b): Compute non–Solenoidal velocity vector field v^*, for given $\left(v^n, v^{n+\frac{1}{2}}, p^n\right)$, such that:

$$\left\{\left(\frac{1}{\Delta t}\left(v^* - v^n\right), v\right) + \frac{1}{2\mathrm{Re}}\left(\nabla\left(v^* - v^n\right), \nabla v\right)\right\} \qquad (8)$$
$$= \left(-p^n - \frac{1}{\mathrm{Re}}\nabla v^n, \nabla v\right) - \left(\left((v.\nabla)v\right)^{n+\frac{1}{2}}, v\right)$$

Stage–2: Calculate pressure–differential $p^{n+1}-p^n$, for given v^* and p^n , such that:

$$\left(\theta\nabla\left(p^{n+1}-p^{n}\right),\nabla q\right)=\frac{-1}{\Delta t}\left(\nabla v^{*},q\right) \qquad (9)$$

Stage–3: Determine velocity vector field at full time–step v^{n+1} for given v^* and $p^{n+1}-p^n$, such that:

$$\left(\frac{1}{\Delta t}\left(v^{n+1}-v^{*}\right),v\right)=\left(\theta\left(p^{n+1}-p^{n}\right),\nabla v\right) \qquad (10)$$

5. <u>THE EFFECT OF PORE–THROAT RATIO ON FLOW CHARACTERISTICS</u>

It is assumed that the value of flow parameters in circular domain remains same, such as pore length taken equal to ***2***□, whilst, for various Pore–Throat ratios, pore radius and throat radius are computed by above equation (01) along axial direction ***z***.

To investigate the effects of Pore–Throat ratios on flow structure, a unit maximum velocity at centre of the computational domain is fixed for all cases. Predicted solutions are demonstrated through streamline projections. Stream function is fixed according to maximum velocity at centre, while, vanishing value of stream function is fixed at solid wall of domain. Vortex intensity is computed through the difference between wall value and the stream function value in the centre of vortex .In core flow, the stream lines are plotted at the difference of 0.05, while, in recirculating region stream lines are plotted at equally spaced according to their stream function values of vortex centre.

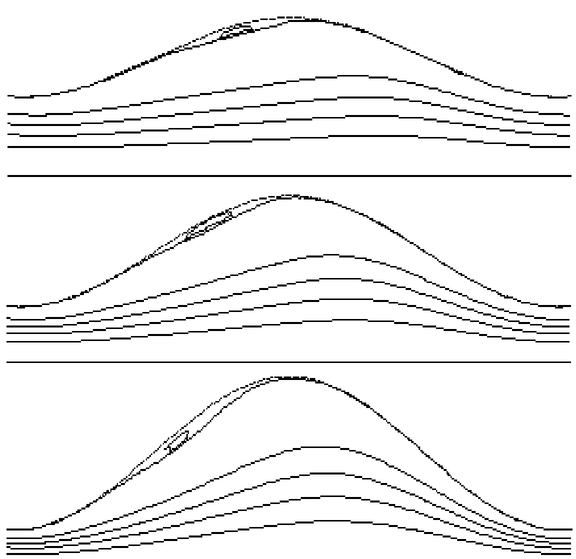

Fig. 3: Streamline contours of vortex development of axisymmetric Pore–Throat problem, with increasing Pore–Throat ratio (from top to bottom 1:2, 1:3, 1:5,) with decreasing inertia (from top to bottom Re = 40, 18, 11).

5.1 Formation of Recirculation Flow Rate (Vortex Development)

For development of recirculating flow rate streamline projections are presented at different Pore–Throat ratios, critical Reynolds numbers are identified in the **(Fig. 3)**. Where, for all Pore–Throat ratios cases, an embryo vortex develops in the upstream of the computational flow domain. At low Pore–Throat ratio of 1:2, vortices develops away from throat and before peak of pore, whereas, as Pore–Throat ratio increase the centre of the embryo vortex shift towards upstream close to upstream throat, this phenomena of formation of recirculation flow rate is illustrated in **(Fig. 3)**.When the ratio is 2, at low value of inertia the fluid velocity is in the upper part of the pore, right close to pore wall. As the Reynolds number is increasing, the fluid velocity in that place reduces evidently and forming vortex (Pilitsis, *et al*. 1991 and Fu-Quan, 2004).

Whilst, in **(Fig. 4)**, graph demonstrate the start of vortex development against critical Reynolds number. It is observed that at small Pore–Throat ratio of 1:2 the start of vortex development is at Reynolds number of forty (Re=40), while for Pore–Throat ratio of 1:5, the start of vortex development is much earlier at Reynolds number of eleven (Re=11) with monotonically decreasing trend with increasing Pore–Throat ratio, subsequently, progresses towards asymptotic behaviour. Whereas, recirculating flow rate is increasing with enhancing Pore–Throat ratio in non–linear fashion.

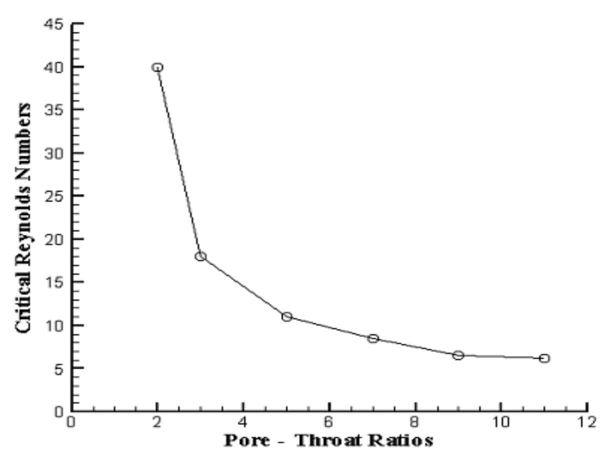

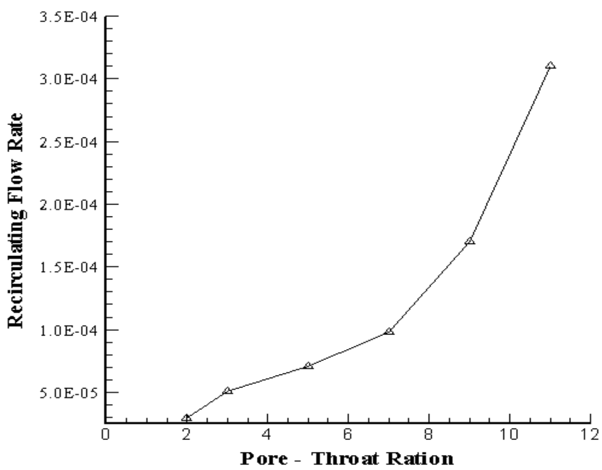

Fig, 4: Graph of vortex development of axisymmetric Pore–Throat problem, with increasing Pore–Throat ratio against decreasing critical Reynolds number (left) and recirculating flow rate (right).

Three different tube models are selected in this study to investigate the effects of various Pore–Throat ratios on various flow characteristics. These Pore–Throat ratios are based on the micro–pore description of genuine reservoir. The various Pore–Throat ratios selected here are 1:2, 1:3 and 1:5 respectively. Since pore radius has small effects on permeability in genuine reservoir and it is generally controlled by throat radius. More over as the pore radius has some changes in low permeability reservoir than throat radius. The précised non–dimensional parameters of each Pore–Throat flow model are obtained through above equation–(01):

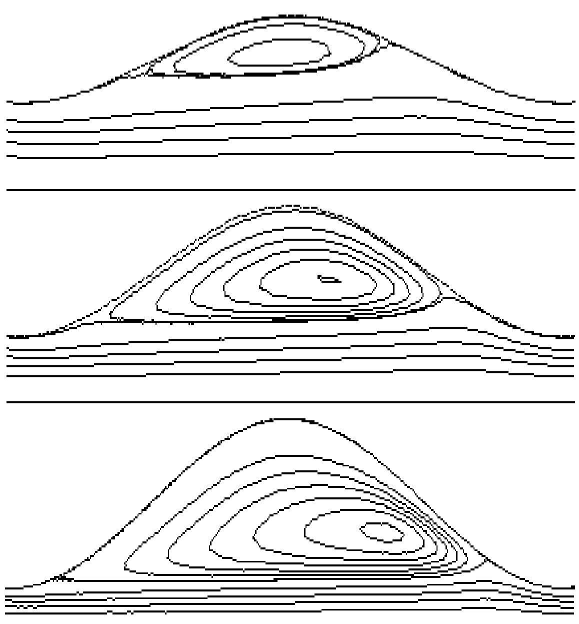

Fig. 5: Streamline projection of axisymmetric Pore–Throat problem at Re = 100, with increasing Pore–Throat ratio from top to bottom (1:2, 1:3 and 1:5).

5.2 Characteristics of Flow Structure, Effects of Inertia

In **(Fig. 5)**, streamline patterns are plotted at Re= 100 shows the flow structure of different Pore–Throat ratios. One can see that, with increasing Pore–Throat ratio a strong recirculating region develops in the centre of pore. As Pore–Throat ratio increases vortex enhancement is observed and strengthening the vortex intensity. Whereas, vortex centre is moving from upstream of pore pushing towards downstream of pore in the vicinity of exit throat. When the Pore–Throat ratio is 1:2, the flow only exists in the vicinity of central line (axis of symmetry) parallel to the throat radius and the fluid velocity at other points in pore is very slow nearly vanishes. Whilst, centre/core flow close to axis of symmetry increases. From stream function's physical significance (the difference in stream function of any two streamlines in plane flow field is equal to volume flow rate per unit thickness), if the ratio is larger, stream function figure is smaller and distance of two adjacent streamlines is smaller. It also represents that if fluid influx and fluid velocity are small, then the volume of relevant fluid passing through the pore space is small. (Balhoff, 2000 and Al-Raoush, *et al*. 2006).

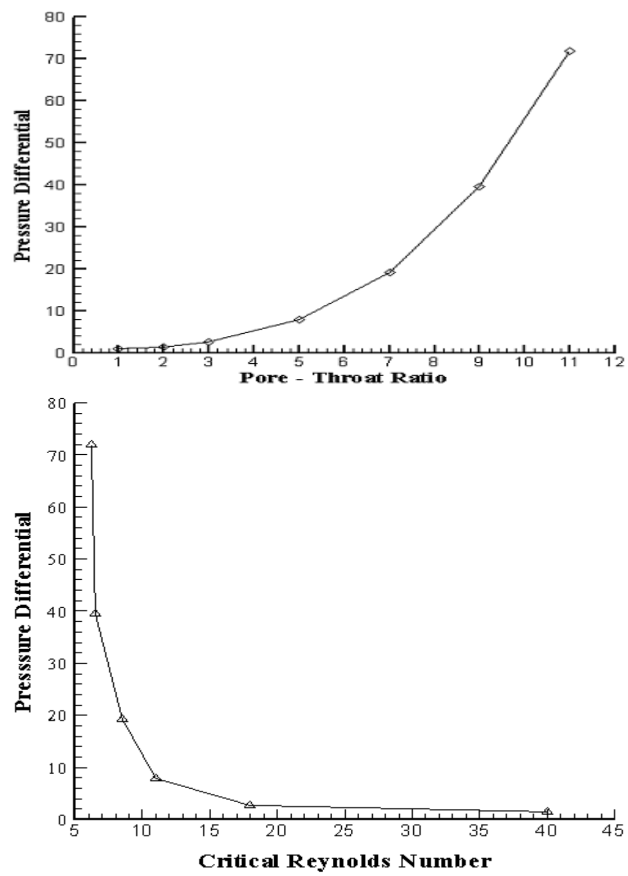

Fig, 6: Graph of the scaled Pressure–Differential of axisymmetric Pore–Throat problem at Re = 100 (left), with increasing Pore–Throat ratio.

5.3 Characteristics Behaviour of Pressure Differential Distribution

In **(Fig. 6)**, the graph of the scaled pressure differential is plotted at Re = 100 with increasing Pore–Throat ratio. Fluid pressure differential is scaled through straight tube of same length. It is clear from the **Figure–06**(on left), that as the Pore–Throat ratio is enhanced, the scaled fluid's pressure differential increases monotonically. At low Pore–Throat ratio, scaled pressure differential slowly increase, whereas, at comparatively high Pore–Throat ratio, scaled pressure differential is increasing rapidly and display exponential tendency. Whilst, at critical Reynolds number the scaled pressure differential display (**Fig.6**) reverse phenomena, i. e., with increasing inertia the scaled pressure differential drops at lowest Pore–Throat ratio, whilst, pressure differential is higher at low value of inertia and larger Pore–Throat ratio. Scaled pressure differential exhibits monotonic decreasing tendency, whereas, at comparatively at higher Reynolds number and lower Pore–Throat ratio the scaled pressure differential approaches to asymptotic state (Lahbabi, and Chang, 1986).

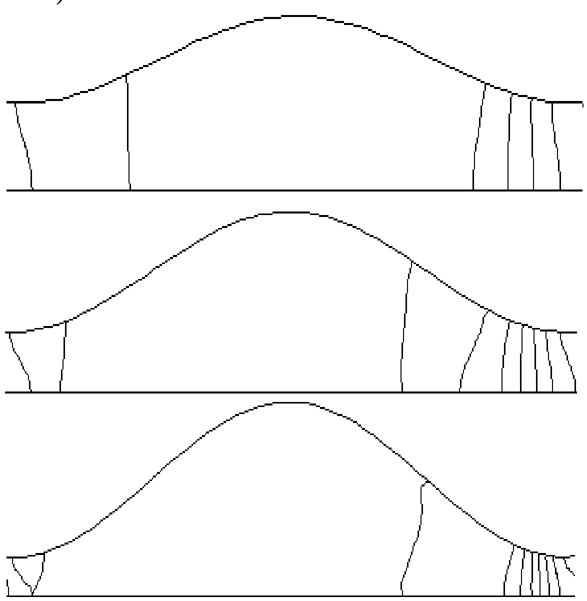

Fig, 7: Pressure contours of axisymmetric Pore–Throat problem at Re = 100, with increasing Pore–Throat ratio

In **(Fig. 7)**, pressure isobars are plotted for Re = 100 with increasing Pore–Throat ratio. It clearly shows that as Pore–Throat ratio is augmented from 1:2 to 1:5, fluid entre from straight tube with unit radius into the first throat, fluid release the pressure inside pore, subsequently, pushes the fluid in the second throat and again it release in the downstream straight tube. For all selected flow model of Pore–Throat pipe at upstream pressure differential increases, whilst, at downstream section it decreases even go in reverse/negative direction.

6. CONCLUSION

To seek the steady–state numerical solutions a Taylor–Galerkin/Pressure–Correction Scheme is Adopting. Numerically computed predictions are compared against other numerically obtained solution and experimental results. Effects of Pore–Throat ratio and influence of inertia (Re) on pressure differential and flow structure investigated. Enhancement of vortices (Q_v) at various Reynolds number is especially focused. The vortex enhancement (Q_v) at different Reynolds number is especially focused. For different Pore–Throat ratio and fluid inertia (Re), start of embryo recirculation region is identified to realise "Critical Reynolds number".

Distinguished calculations of 1:2, 1:3 and 1:5 Pore–Throat rations separately, it is concluded that when the ratio increase or throat radius reduced and pore radius increase, then internal–pore velocity of fluid will decrease and a recirculating region develops. This recirculating region grows and occupy large area of pore region, subsequently, strengthening the vortex intensity at high value of inertia and almost grapes whole pore region. Whereas, in core flow, the velocity of the fluid increases with increasing inertia.Predicted solutions illustrate the association between recirculating flow–rate and pressure differential appearing in agreement with Navier–Stokes equations.

7. ACKNOWLEDGEMENT

Authors would like to thanks the Department of Petroleum Engineering, University of Stavanger, Norway, Institute of Computer Engineering, University of Duisburg-Essen, Campus Duisburg, Germany and Department of Mathematics, Shah Abdul Latif University, Khairpur Pakistan, for providing the opportunity to carry out this research work and computing facility.

REFERENCES:

Al–Raoush, R., K. A. Alshibli, (2006), "Distribution of Local Void Ratio in Porous Media Systems from 3D X–Ray Micro Tomography Images", [J]. Physica A: Statistical Mechanics and its Applications, 361(2), 441–456.

Baloch, A., (1994). Numerical Simulation of Complex Flows of Now–Newtonian Fluids, PhD Thesis, University of Wales, Swansea, UK.

Baloch, A., P. Townsend, M. F. Webster, (1995), "On the Simulation of Highly Elastic Complex Flows", J. Non–Newtonian Fluid Mech., Vol. 59(2/3), 111–128.

Baloch, A., A. S. Memon, (2007), "Simulation of Corrugated Tube Flow of Non–Newtonian Fluids", MUETJET, Vol. 26(1), 19–32.

Baloch, Z. A. K., M. E. Baloch, H. Shaikh, M. A. Shar, (2013), "Computer Simulation of Lid Driven shallow Cavity Flows: Effects of Fluid Inertia and Aspect Ratios", Sindh Univ. Res. Jour. (Sci. Ser.), Vol.45 (2), 277–280.

Baloch, Z. A. K., M. E. Baloch, R. A. Memon, H. Shaikh, (2014), "Computer Simulation of Lid Driven Deep Cavity Flow" , Sindh Univ. Res. Jour. (Sci. Ser.), Vol.46 (4), 457–460.

Bear, J., (1988), "*Dynamics of Fluids in Porous Media*", New York, Elsevier, 1972, (reprinted by Dover Publications).

Balhoff, M., (2000), "Modelling the Flow of Non–Newtonian Fluids in Packed Beds at the Pore Scale", Ph.D. thesis in the department of Chemical Engineering Southfield, Michigan.

Fu–Quan, S., (2004), "Research of the Size Effect of Liquid Flow in Low Permeability Porous Media and Micro–channels", J. Nature Magazine, Vol. 26(3), 128–131.

Gravesen, P., J. Branebjerg, O. S. Jensen, (1993), "Micro Fluidics–A Review", J. of Micromechanics and Micro engineering, Vol. (3), 168–182.

Hassanipour, F., J. Lage, (2007), "The Effect of a Porous Medium on the Flow of a Liquid Vortex", Int. J. Eng., 3(6), 587–596.

Harley, J. C., Y. F. Huang, H. H. Bau, (1995), "Gas Flow in Micro–Channels", J. Fluid Mech., Vol. (284), 257–274.

Jicheng, Z., Q. Guixue, M. U. Wenzhi, S. Kaoping, (2010), "Investigation on the Characteristics of Flow in Expansion–Contraction Channel of Low Permeability Reservoir", Journal of Physical and Numerical Simulation of Geotechnical Engineering, DOI: 10. 5503/J. PNSGE.

Kandlikar, S. G. (2002), "Fundamental Issues Related to Flow Boiling in Mini Channels and Micro Channels", J. Exp. Therm. Fluid Sci., Vol. 26, 38–47.

Lahbabi, A., H. C. Chang, (1986), "Flow in periodically Constricted Tubes: Transition to Inertial and Unsteady Flows", J. Chemical Engineering Society, Vol. 41, 2487–2505.

Makihara M., K. Sasakura, A. Nagayama, (1993), "Flow of liquids in micro–capillary tube consideration to application of the Navier Stokes equations", J. of the Japan Society of Precision Engineering/ SeimitsuKogakuKaishi, 59 (3), 399–404.

Mala, G. M., L. Dong-Qing, (1999), "Flow Characteristics of Water in Micro Tubes", Int. J. of Heat and Fluid Flow, Vol. (20), 142–148.

Memon, R. A., Z. A. K. Baloch, H. Shaikh, S. B. Shah, A. Baloch, (2015), "Numerical Study of Stresses of Rotating Mixing Flow within a Container", Sindh Univ. Res. Jour. (Sci. Ser.) Vol.47 (1), 45–48.

Pfahler, J., J. Harley, H. Bau, (1990), "Liquid Transport in Micronand Submicron Channels", J. Sensors and Actuators, A2-A23, 431–434.

Pilitsis, S., A. Souvaliotis, A. N. Beris, (1991), "Viscoelastic Flow in a Periodically Constricted Tube: The Combined Effect of Inertia, Shear Thinning and Elasticity", J. Rheology, Vol. 35(4), 605–646.

Qureshi, A. L., A. Baloch, (2013), "Finite Element Simulation of Suspended Sediment Transport: Development, Validation of Application to Photo minor, Sindh, Pakistan", Advances in River Sediment Research. Fukuoka *et al*. (Eds.), Taylor and Francis Group, London, 1825–1832.

Shah, S. B., H. Shaikh, M. A. Solangi, A. Baloch, (2013), "Numerical Simulation of Flow through a Periodically Constricted Tube: Effects of Inertia and Undulation on Flow Structure" Sindh Univ. Res. Jour. (Sci. Ser.) Vol.45 (1), 35– 40.

Shah, S. B., H. Shaikh, M. A. Solangi, A. Baloch, (2014), "Computer Simulation of Fibre Suspension Flow through a Periodically Constricted Tube", Punjab University Journal of Mathematics (ISSN 1016-2526), Vol. 46(2), 19–34.

Shaikh, H., S. B. Shah, M. A. Solangi, A. Baloch, (2013), "Effects of Local Inertia in the Expansion Channel Filled with Porous Media: A Finite Element Analysis", Sindh Univ. Res. Jour. (Sci. Ser.), Vol. 45(2), 207–212.

Shaikh, H., S. B. Shah, M. A. Solangi, A. Baloch, (2012), "A Computer Simulation of Flow of Newtonian Fluid through Backward Step Channel", Sindh Univ. Res. Jour. (Sci. Ser.), Vol. 44(4), 703–708.

Solangi, M. A., H. Shaikh, R. B. Khokhar, A. Baloch, (2013), "Numerical Study of Newtonian Blood Flow through a Plaque Deposited Artery", Sindh Univ. Res. Jour. (Sci. Ser.), Vol. 45 (1), 79–82.

Song, R., J. Liu, (2014), "Advances in Microscopic Pore Structure Modelling of Rock" Journal of EJGE, china, Vol. 19. 47–57.